REPORTS

Compositional Trends in Rock-Forming Elements of Comet Halley Dust

M. N. Fomenkova,* J. F. Kerridge, K. Marti, L.-A. McFadden

The VEGA 1 and 2 spacecraft flew by comet P/Halley in 1986 carrying, among other instruments, two mass spectrometers to measure the elemental composition of dust particles emitted from the comet. Most particles seem to be a mixture of silicates of variable magnesium-iron composition and organic matter. Comprehensive study of data and consideration of the mass of dust particles reveal cometary grains of "unusual" composition: magnesium-rich and iron-rich particles. Magnesium-rich particles are most likely magnesium carbonates, which could not have formed under conditions of equilibrium condensation but rather require formation by aqueous alteration. The composition of the iron-rich particles can also be related to secondary processes in the comet.

Comets are believed to contain low-temperature, primitive solar nebular material from the early formation of the solar system. During the exploration of comet Halley in 1986, an international fleet of five spacecraft acquired in situ measurements at various distances from the comet nucleus and extensive ground-based observations were also made. Two Soviet VEGA spacecraft flew as close as 8000 km to the comet nucleus. Time-of-flight dust-impact mass spectrometers named PUMA-1 and PUMA-2 (*1, 2*) onboard the spacecraft measured more than 2500 mass spectra of comet Halley dust particles. In this report, we analyze these data and discuss their implications for our understanding of comets.

The information obtained by PUMA-1 and PUMA-2 is specific for the region of the coma that was sampled. The results are quite alike and have similar trends, but there are some differences and it is not clear to what extent the data reflect the average composition of comet Halley. The total mass of measured dust particles is about 0.5 ng, which is comparable to the mass of only one interplanetary dust particle (IDP) (collected from the stratosphere). It may represent a good sample of Halley if the comet is composed primarily of very small grains and is internally homogeneous, for dust particles were measured along the flyby trajectory and were not all taken from the same place but were derived from a large volume of the parent body. The problem of representativeness and reliability of results obtained from flyby measurements should be kept in mind in evaluating far-reaching conclusions about the chemistry of comets, processes in the solar nebula, and the galactic history of elements made from investigation of less than 1 ng of the Halley dust.

Dust particles from the comet Halley dust envelope collided with the silver target of the instrument with a relative velocity of about 80 km/s and were ionized by hypervelocity impact. On passing through a time-of-flight analyzer, ions were separated according to their mass-to-charge (*m/q*) ratio. The resulting spectrum was recorded by a secondary electron multiplier. Most of the analyzed ions were singly charged atomic ions. About 10% of the spectra were measured by sampling each 67 ns and transmitted without compression; these spectra contain information about peak shapes [see figures in (*1*)]. The other 90% were compressed onboard so that only amplitude (number of ions) and position (time of flight corresponding to atomic mass) of each peak are available [examples in (*3*)].

To calculate elemental abundances from ion abundances, it is necessary to introduce corrections for ionization yields and registration efficiencies. Laboratory calibration of PUMA instruments was impossible because there are no facilities to accelerate dust grains to 70 km/s. Theoretical estimates used were based either on extrapolation of laboratory experiments at velocities ≤ 10 km/s and yields of secondary ion emission processes (*4*) or on the calculation of a hydrodynamical model of expansion of a plasma cloud originating from hypervelocity collision of a dust particle with the target of the instrument (*5, 6*).

Attempts were made (*3, 6, 7*) to determine ion and elemental abundances of H, C, N, O, Na, Mg, Al, Si, S, Cl, K, Ca, Ti, Cr, Fe, and Ni in cometary grains. Ion ratios were given (*6*) for 2204 compressed spectra of PUMA-1, without selection by quality. Seventy-nine uncompressed spectra of PUMA-1 were considered (*7*), which is hardly a representative sample (*8*). Elemental abundances based on ionization efficiencies (*4*) agreed with carbonaceous chondrite abundances (*9*) within a factor of 2. In other work, 433 compressed spectra of PUMA-1 selected according to inferred quality were considered (*3*). The Mg/Si, Fe/Si, and Fe/Mg ratios for individual dust particles were multiplied by constant correction factors such that histograms of corrected ratios peaked at the proper solar ratios.

In all these studies, the mass of each dust grain was not considered, although it is clear that larger grains should contribute more to the bulk abundance. In (*6, 7*) all particles were given equal weight in producing bulk abundances, thus overestimating the contribution of the smallest particles. Masses of dust particles were determined to be in the range 5×10^{-17} to 5×10^{-12} g (*10*). The bulk ion abundances for 2031 compressed spectra of PUMA-1 and 517 compressed spectra of PUMA-2 were recalculated (*11*) by assuming that the contribution of each particle was proportional to its mass. The resulting abundances agreed rather well with solar abundances (*9*) when no additional corrections were applied. Significant differences were evident in the composition of heavy ($>10^{-13}$ g) and light ($<10^{-15}$ g) grains and there was also a different mass dependence of the grain composition for different particle types. The models (*4, 5*) do not agree with these observed differences; their common shortcoming is that they predict constant ionization efficiencies independent of the mass and density of particles.

There are two major differences between the present approach and earlier ones (*3, 6, 7*): In this study (i) the largest available (*11*) sample of cometary matter is studied (1868 compressed spectra of PUMA-1 and 500 compressed spectra of PUMA-2); and (ii) dust grains are considered in three mass ranges: $<10^{-15}$ g, small; 10^{-15} g to 10^{-13} g, medium; and $>10^{-13}$ g, large.

We attempted a systematic and quantitative classification of cometary grains into three major types based on their composition. If the ratio of C to any rock-forming elements (Mg, Si, Fe, Ca) was >10, a particle was categorized as "CHON," for composed mainly at least of carbon, possibly hydrogen, oxygen, and nitrogen. If this ratio was <0.1, a particle was included in the group "Rock"; the remainder are "Mixed" particles.

As pointed out earlier (*3, 7*), in some spectra the apparent isotope ratios ^{24}Mg/^{25}Mg and ^{24}Mg/^{26}Mg are considerably larger than the normal ratios of 7.8 and 7.0, respectively. Such large isotopic anomalies of Mg have never been observed in meteorites or IDP and therefore are probably due to interference by molecular ions [for example, C_2^+ (*7*)]. For this reason, we made three variants of the classification:

M. N. Fomenkova, Space Research Institute, Academy of Sciences, Moscow, Russia, and California Space Institute, University of California San Diego, La Jolla, CA 92093.
J. F. Kerridge and K. Marti, Department of Chemistry, University of California San Diego, La Jolla, CA 92093.
L.-A. McFadden, California Space Institute, University of California San Diego, La Jolla, CA 92093.

*To whom correspondence should be addressed.

Table 1. Classification of comet Halley dust particles. *N*, number of spectra.

Type	PUMA-1		PUMA-2	
	N	Total mass (10^{-12} g)	*N*	Total mass (10^{-12} g)
CHON	464	113	51	8
Mixed	974	226	288	86
Rock	430	21	161	25
All	1868	360	500	120

Variant 1: All ions at $m/q = 24$ were taken as ^{24}Mg.

Variant 2: If the ratio α of ions with $m/q = 24$ to the geometric mean $(^{25}\mathrm{Mg}^{26}\mathrm{Mg})^{1/2}$ was higher than 15 (twice the terrestrial value), then the Mg abundance was based on the minor isotopes and set equal to 7.2 times $(^{25}\mathrm{Mg}^{26}\mathrm{Mg})^{1/2}$. The number of such corrected spectra is 392 (21%) for PUMA-1 and 66 (13%) for PUMA-2.

Variant 3: The same procedure was used as for variant 2, but for $\alpha \geq 10$. The number of such corrected spectra is 624 (33%) for PUMA-1 and 80 (16%) for PUMA-2.

These variants resulted in insignificant differences in the classification: <2% of spectra between variants 1 and 2 [shown in Table 1 (*12*)], <1% of spectra between variants 2 and 3. Differences are minor because by definition the ratios of C to Mg in the extreme groups CHON and Rock differ at least by two orders of magnitude, which is much more than the introduced corrections.

As shown in Table 1, CHON particles are relatively more abundant in PUMA-1 than in PUMA-2 data. Performance of the PUMA-2 instrument was affected by malfunctions in the onboard power supply; this led to nonuniform sampling of dust along the trajectory and the absence of spectra of the smallest particles ($<10^{-16}$ g). This circumstance may explain the difference between PUMA-1 and PUMA-2 data. On the other hand, production rates of some gaseous organic species in the coma were shown (*13*) to be related to the rotational phase of the nucleus. If so, the nucleus may be inhomogeneous in composition. On the date of the PUMA-2 flyby, a different region of the nucleus (containing less organic material) was emitting dust particles than during the PUMA-1 flyby, which is consistent with ground-based observations of the coma made on the same dates.

In PUMA-1 data CHON particles represent about 25% of all particles. On average, in the mass range covered they are more massive than particles of the other two groups. CHON particles are supposed (*14*) to be the main sources of some species ($C_3H_3^+$, C_3H^+) in the coma of comet Halley. Rock particles represent about 23% of the dust population sampled. There is compositional variability within each category of particles. Mineral phases inferred in particles of Rock and Mixed types (*3, 7, 15*) are mostly magnesium silicate and various Fe-containing phases. On the ternary diagram Mg + Fe, Si, C the major trend corresponds to a solar (Mg + Fe)/Si ratio 2:1, lending considerable support to our calibration procedure. The trend with 1:1 ratio indicating pyroxene stoichiometry is also observed. We assume that Mixed particles consist of a mixture of variable Mg/Fe silicates and organic matter. Spectra containing H, possibly O, and rock-forming elements, but no C were interpreted (*16*) as evidence of layer silicates in cometary dust particles. They are more frequent among small particles.

Earlier analysis suggested that Mg is enriched in some of the smallest cometary grains (*11*), and (Mg, C, O)-grains were found among the particle impact analyzer (PIA) data (*17*). Also, some spectra of gram-sized dust material from the Orionid meteor shower associated with comet Halley demonstrated the surprisingly strong lines of neutral Mg near 5176 and 3833 Å (*18*), which suggests a high abundance of Mg in these meteors. This feature has not been observed in meteor showers associated with other comets.

The Mg/Si variation (Fig. 1) with mass and particle type either is an artifact of measurement or reflects actual differences in elemental composition, hence indicating particles of different nature and possibly different origin. The first possibility has been evaluated in a detailed model of the dynamics and kinetics of plasma-cloud formation by hypervelocity impact of a particle on a silver target (*19*). Plasma processes in the instrument depend on (i) the number of particles in plasma cloud, which is roughly proportional to particle mass, and (ii) initial conditions of collision (temperature and pressure), which depend on particle density. Differential ionization efficiencies for particles of different type and mass may cause different ion ratios for the same original elemental ratios. Calculations (*19*) demonstrated that, for initially equal elemental concentrations of Mg and Si, the ratio of quenched ion concentrations Mg^+/Si^+ for particles of mass 10^{-12} g equals 1.0, independent of their density. For particles of mass 10^{-15} g, it equals 1.4 for fragile particles (density 0.4 g/cm^3) and 2.0 for dense particles (3.0 g/cm^3). The model shows that variations in the Mg^+/Si^+ ratio in Fig. 1 can be explained, in part, in terms of plasma effects. The correction procedure used in (*4*) applied to large particles would shift the Mg/Si bulk ratio toward a value of ~0.3, considered unrealistic for solar system material.

However, in some spectra of cometary dust particles the Mg^+/Si^+ ratio is more than 8 (twice the average in Fig. 1) and cannot be easily explained by any model (*6, 7, 18*). Thus, a spectrum was defined as Mg-rich if

$$^{24}\mathrm{Mg}/^{28}\mathrm{Si} > 8,\ ^{24}\mathrm{Mg}/^{56}\mathrm{Fe} > 1, \text{ and}$$

$$^{24}\mathrm{Mg}/^{40}\mathrm{Ca} > 1$$

We considered spectra separately in each grain size range and for the three variants of the ^{24}Mg assignment described earlier. For PUMA-1 data, the number of Mg-rich spectra for variant 1 in all mass ranges is about 1.6 times those for variant 2 [shown in Table 2 (*14*)] and 1.8 times those for variant 3. For PUMA-2 data the number of Mg-rich spectra is the same for all variants because in Mg-rich spectra obtained by PUMA-2 the Si ions are usually below the detection limit.

The model of plasma formation by hypervelocity impact predicts a significant enrichment of Mg in small particles, but Mg-rich particles are observed in all mass

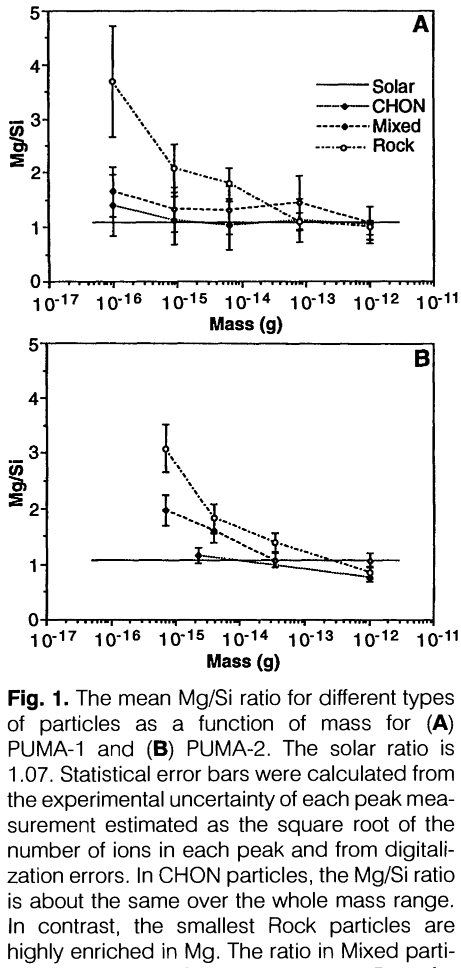

Fig. 1. The mean Mg/Si ratio for different types of particles as a function of mass for (**A**) PUMA-1 and (**B**) PUMA-2. The solar ratio is 1.07. Statistical error bars were calculated from the experimental uncertainty of each peak measurement estimated as the square root of the number of ions in each peak and from digitalization errors. In CHON particles, the Mg/Si ratio is about the same over the whole mass range. In contrast, the smallest Rock particles are highly enriched in Mg. The ratio in Mixed particles is between these two groups. Data for PUMA-2 demonstrate the same tendency, but the absence of data for the smallest particles makes it less noticeable.

Table 2. Number (N) of Mg-rich particles as a function of mass. Percentages reflect the number of Mg-rich spectra in each mass range. In PUMA-2 data the proportion of Mg-rich particles diminishes as the mass of the particles increases but in the statistically more reliable PUMA-1 data it is about the same independent of particle mass.

Mass	PUMA-1		PUMA-2	
	N	%	N	%
$<10^{-15}$ g	63	12.0	37	28.7
10^{-15} to 10^{-13} g	50	6.1	29	11.1
$>10^{-13}$ g	51	9.9	8	7.2
All	164	8.8	74	14.8

Table 3. Number (N) of Fe-rich particles as a function of mass. Percentages are relative to the total number of spectra in each mass range. Iron-rich particles are more abundant among particles of larger mass.

Mass	PUMA-1		PUMA-2	
	N	%	N	%
$<10^{-15}$ g	35	6.6	6	4.7
10^{-15} to 10^{-13} g	32	3.9	14	5.4
$>10^{-13}$ g	54	10.5	13	11.7
All	121	6.5	33	6.6

Table 4. Chemical composition of Fe-rich particles. N, number of spectra.

	PUMA-1		PUMA-2 (N)
	N	N with Ni (%)	
Metal (Fe/S > 10.0; Fe/Si > 10.0)	21	43	8
Sulfides (Fe/S < 10.0; S/Si > 5.0)	35	26	10
Silicates (Fe/Si < 10.0; Si/S > 5.0)	15	40	4
Other	50	34	11

ranges. This finding suggests that a population of Mg-rich grains indeed may be present in comet Halley dust. These grains are probably magnesium carbonates rather than magnesium sulfates as the C/S ratio is more than 2.0 in about 58% of the Mg-rich spectra of PUMA-1 and less than 0.5 in only 8% of spectra (46% and 8% for corresponding PUMA-2 data). The proportion of magnesium carbonates is about 7% by weight [of all measured spectra, see (*12*)] in PUMA-1 data and about 1% by weight in PUMA-2 data.

A weak emission feature at 6.8 μm attributed to carbonates was observed in comet Halley (*20*). Carbonates (and layer silicates) are minor but persistent phases in anhydrous chondritic porous IDP (*21*), which are supposed (*22*) to originate from short-period comets. In CI and CM meteorites magnesium carbonates are abundant; they likely formed as a result of aqueous activity on the CI and CM parent bodies (*23*).

Minerals with high Mg/Si ratio could not have formed by equilibrium condensation in the solar nebula (*24*) but can be produced by secondary processing such as aqueous alteration. The presence of layer silicates in cometary grains (*16*) also raises the possibility of hydration in their history, which would not have occurred in the nebula (*25*). Hydrated phases in comet Halley dust are consistent with formation in situ by hydrocryogenic alteration. Such activity in nuclei of active short-period comets has been hypothesized (*21*) to take place in interstitial water layers at dust-ice interfaces below the melting point of water-ice. If this was the case, then melted water was only a local phenomenon. On the other hand, the 6.8-μm feature was observed in protostellar spectra, which raises the possibility that cometary carbonates may be primary components (*26*).

In another 34% of the Mg-rich spectra of PUMA-1 and 46% of the Mg-rich spectra of PUMA-2, the Mg/C and Mg/S ratios are >10. These data may suggest the presence of periclase or brucite, or both. These minerals are present in some meteorites and IDP (*27*), but only as minor phases.

Both Fe and Ni were identified in emission spectra of sun-grazing comets where radiation temperatures exceed 10^3 K and thus can vaporize the refractory components of dust (*28*). Pure metal grains containing only Fe and Ni are well known in meteorites, but the question about the presence of unoxidized metal grains and the possibility of their survival in a cometary environment has remained unclear. We investigated Fe-rich spectra of comet Halley dust particles defined as

$$^{56}\mathrm{Fe}/^{24}\mathrm{Mg} > 1,\ ^{56}\mathrm{Fe}/^{28}\mathrm{Si} > 1, \text{ and}$$

$$^{56}\mathrm{Fe}/^{40}\mathrm{Ca} > 1$$

Spectra with a major peak at mass 56 but without a peak at mass 54 were rejected. The mean ratio of mass 54/56 in statistically reliable spectra (amplitude of mass 56 is >100) is equal to 0.06 ± 0.02 and is similar to the ^{54}Fe/^{56}Fe isotope ratio.

Iron-rich particles do exist in cometary dust (Table 3), and there is evidence for the presence of metal, iron oxide, iron sulfides, Fe-rich silicates, and mixtures of these minerals in cometary grains (Table 4).

In meteorites nearly all metal particles contain Ni (*29*). The percentage of Fe-rich grains with Ni is about one-third, the same for all chemical groups of particles (the mean Ni/Fe ratio in spectra with ^{56}Fe > 100 equals 0.14 ± 0.03) (Table 4). These data suggest that only a fraction of the Fe-rich particles may be pure metal while others are iron oxide (*30*) or mixed phases with Fe-Ni metal inclusions. The presence of Fe in oxidized form would again point toward aqueous alteration (*31*).

Most of the comet Halley dust particles demonstrate chondritic composition and are mixtures of various primary silicate phases. There is also evidence for minor populations of Mg-rich and Fe-rich particles, which possibly have a secondary origin.

REFERENCES AND NOTES

1. J. Kissel *et al.*, *Nature* **321**, 280 (1986).
2. V. M. Balebanov, G. A. Scuridin, E. V. Vorontzova, Eds., *Venus-Halley Mission* (Lous-Jean, Paris, 1984), pp. 88–93.
3. M. E. Lawler, D. E. Brownlee, S. Temple, M. M. Wheelock, *Icarus* **80**, 225 (1989).
4. J. Kissel and F. R. Krueger, *Appl. Phys. A* **42**, 69 (1987).
5. N. A. Inogamov, *Dokl. Acad. Nauk SSSR* **277**, 1377 (1986).
6. Y. Langevin *et al.*, *Astron. Astrophys.* **187**, 761 (1987).
7. E. K. Jessberger, A. Cristoforidis, J. Kissel, *Nature* **332**, 691 (1988).
8. A. H. Delsemme, in *Comets in the Post-Halley Era*, R. L. Newburn *et al.*, Eds. (Kluwer Academic, Dordrecht, Netherlands, 1991), pp. 377–428.
9. E. Anders and N. Grevesse, *Geochim. Cosmochim. Acta* **83**, 197 (1989).
10. M. N. Fomenkova *et al.*, *Lunar Planet. Sci. Conf.* **22**, 397 (1991).
11. L. M. Mukhin *et al.*, *Nature* **350**, 480 (1991). In comparison with this work, 163 spectra of PUMA-1 and 17 spectra of PUMA-2 were rejected in the present study as being of poor quality (high noise level or narrow dynamic range of amplitudes because of saturation effects in the data-acquisition system).
12. Usually, we refer to variant 2 in our discussion, for isotopic ratios are considered to be accurate within a factor of 2 as a result of the low amplitudes of ^{25}Mg and ^{26}Mg and hence the lower accuracy of these values.
13. M. J. Mumma, D. Reuter, K. Magee-Sauer, *Bull. Am. Astron. Soc.* **22**, 1088 (1990).
14. A. Korth *et al.*, *Nature* **337**, 53 (1989).
15. Yu, P. Dikov *et al.*, *Adv. Space Res.* **9** (no. 3), 253 (1989).
16. F. J. Rietmeijer, L. M. Mukhin, M. N. Fomenkova, E. N. Evlanov, *Lunar Planet. Sci. Conf.* **20**, 904 (1989).
17. B. C. Clark, L. W. Mason, J. Kissel, *Astron. Astrophys.* **187**, 779 (1987).
18. I. Halliday, *ibid.*, p. 921.
19. A. Dychne and S. Kozochkin, *Tech. Rep. 26-08-91* (Space Research Institute, Moscow, 1991).
20. J. D. Bregman *et al.*, *Astron. Astrophys.* **187**, 617 (1987).
21. F. J. Rietmeijer, *Earth Planet. Sci. Lett.* **102**, 148 (1991).
22. L. S. Shramm, D. E. Brownlee, M. M. Wheelock, *Meteoritics* **24**, 99 (1989).
23. K. Fredriksson and J. F. Kerridge, *ibid.* **23**, 35 (1988); T. E. Bunch and S. Chang, *Geochim. Cosmochim. Acta* **44**, 1543 (1980).
24. J. F. Kerridge, *Proc. Lunar Planet. Sci. Conf.* **10**, 989 (1979).
25. R. G. Prinn and B. Fegley, in *Origin and Evolution of Planetary and Satellite Atmospheres*, S. K. Atreya, J. B. Pollack, M. S. Matthews, Eds. (Univ. of Arizona Press, Tucson, 1988), pp. 78–136.
26. S. A. Sandford and R. M. Walker, *Astrophys. J.* **291**, 838 (1985).
27. E. K. Zinner, C. Caillet, A. E. Goresy, *Lunar Planet. Sci. Conf.* **20**, 1245 (1989); M. E. Zolensky and D. J. Lindstrom, *Proc. Lunar Planet. Sci. Conf.* **22**, 161 (1992).

28. C. Arpigny, in *Elements and Isotopes in the Universe* (22nd Colloquium in Astrophysics, University of Liège, Liège, 1979), pp. 189–197.
29. D. Sears and R. T. Dodd, in *Meteorites and the Early Solar System*, J. F. Kerridge and M. S. Matthews, Eds. (Univ. of Arizona Press, Tucson, 1988), pp. 3–31. Rare exceptions consist of fine beads of pure Fe exsolved from olivines in chondrites during reheating in a reducing environment [see A. Kracher, E. R. D. Scott, K. Keil, *J. Geophys. Res.* **89**, B559 (1984)].
30. The complete loss of signal for oxygen in some spectra was reported as a peculiar feature of PUMA instruments by E. N. Evlanov *et al.*, in *Chemistry in Space*, J. M. Greenberg and V. Pirronello, Eds. (Kluwer Academic, Dordrecht, Netherlands, 1991), pp. 383–397.
31. J. F. Kerridge, A. L. Mackay, W. V. Boynton, *Science* **205**, 395 (1979).

32. M.N.F. and L.-A.M. thank California Space Institute and S. Ride for support during the completion of this work. This work was supported in part by National Aeronautics and Space Administration (NASA) grants. J.F.K. was supported through NASA grant NAGW 347. We thank D. E. Brownlee for his constructive comments as a referee.

4 February 1992; accepted 14 July 1992

X-ray Laser Microscopy of Rat Sperm Nuclei

L. B. Da Silva,* J. E. Trebes, R. Balhorn, S. Mrowka, E. Anderson, D. T. Attwood, T. W. Barbee, Jr., J. Brase, M. Corzett, J. Gray, J. A. Koch, C. Lee, D. Kern, R. A. London, B. J. MacGowan, D. L. Matthews, G. Stone

The development of high brightness and short pulse width (<200 picoseconds) x-ray lasers now offers biologists the possibility of high-resolution imaging of specimens in an aqueous environment without the blurring effects associated with natural motions and chemical erosion. As a step toward developing the capabilities of this type of x-ray microscopy, a tantalum x-ray laser at 44.83 angstrom wavelength was used together with an x-ray zone plate lens to image both unlabeled and selectively gold-labeled dried rat sperm nuclei. The observed images show ~500 angstrom features, illustrate the importance of x-ray microscopy in determining chemical composition, and provide information about the uniformity of sperm chromatin organization and the extent of sperm chromatin hydration.

Historically, advances in imaging technology have led to new and exciting results in the field of biology. Today, electron microscopy (EM), optical microscopy (OM), and atomic force microscopy (AFM) are necessary tools for biologists and biochemists around the world. These techniques offer high resolution (<20 Å for EM/AFM) of prepared specimens or lower resolution (~2000 Å for OM) of specimens in their natural environment. An alternative imaging technology that is now becoming available is x-ray microscopy, which offers the possibility of high-resolution imaging (~200 to 300 Å) of specimens in their natural environment. In addition, x-ray microscopy with the use of x-rays of different wavelengths can be used to probe the interior of living cells. This is currently practical only with OM.

L. B. Da Silva, Department of Physics, University of California at Berkeley, Berkeley, CA 94720.
J. E. Trebes, R. Balhorn, S. Mrowka, T. W. Barbee, Jr., J. Brase, M. Corzett, J. A. Koch, C. Lee, R. A. London, B. J. MacGowan, D. L. Matthews, G. Stone, Lawrence Livermore National Laboratory, P.O. Box 808, Livermore, CA 94550.
E. Anderson and D. T. Attwood, Center for X-ray Optics, Lawrence Berkeley Laboratory, Berkeley, CA 94720.
J. Gray, Division of Molecular Cytometry, University of California at San Francisco, San Francisco, CA 94143.
D. Kern, IBM T. J. Watson Research Center, P.O. Box 218, Yorktown Heights, NY 10598.

*To whom correspondence should be addressed.

To date, x-ray microscopy has been developed and demonstrated by several groups around the world. Resolutions near the diffraction limit have been reported by Jacobsen *et al.* (*1*) and Meyer-Ilse *et al.* (*2*); both groups used synchrotron radiation to image biological systems. X-rays generated in a laser-produced plasma were recently used by Tomie *et al.* (*3*) to produce 0.5-ns flash contact x-ray images of a hydrated sperm cell with a spatial resolution of ~1000 Å. Extending the use of laser plasma sources to imaging microscopy where chromatic aberrations necessitate the use of narrow bandpass optics will reduce signal levels. A narrow band 182 Å x-ray laser was previously used to produce contact x-ray micrographs of dry cervical cancer cells (*4*). However, only recently have x-ray lasers with wavelengths near and inside the water window (23 to 44 Å) been developed (*5*) that have sufficient output energy for microscopy of a wide range of biological objects. We recently demonstrated x-ray imaging using such an x-ray laser as the illuminator (*6*). The key advantage of an x-ray laser is that its high brightness and short duration allow images to be made with a single ~200-ps exposure. This eliminates the problems associated with motion blurring and radiation-induced chemical decomposition of the specimen. In addition, the quasi-monochromatic property of x-ray lasers makes them well suited to x-ray optics. In this report we discuss images taken of dried rat sperm nuclei with the use of this short-pulse x-ray laser source.

The x-ray imaging microscope we used is shown schematically in Fig. 1. X-rays from a nickel-like tantalum collisionally pumped x-ray laser (*7*) operating at 44.83 Å are collected and focused onto a specimen that is then imaged in transmission by a Fresnel zone plate lens (*8*) on a microchannel plate detector. The x-ray laser was generated by irradiation of a 3.5 cm long, 2000 Å thick plastic foil coated with 900 Å of tantalum with two cylindrically focused visible light (0.53 μm) laser beams. The heated foil explodes to form a high-temperature plasma with low-density gradients (*9*). For our experiment, two optical beams from the Nova Laser at Lawrence Livermore National Laboratory were used to generate an intensity on target of 3.0×10^{14} W/cm^2 for a duration of 500 ps (*7*). The x-ray laser originates from an ~100-μm-diameter gain region at the center of the plasma and has a beam divergence of 10 mrad [full width at half maximum (FWHM)]. The output energy is ~10 μJ in a 200-ps (FWHM) pulse that corresponds to a brightness of 10^{21} photons/(s mrad^2 mm^2 0.01% bandwidth). This is four orders of magnitude brighter than the X-1A beam line at the National Synchrotron Light Source, currently the world's brightest soft x-ray synchrotron beam line.

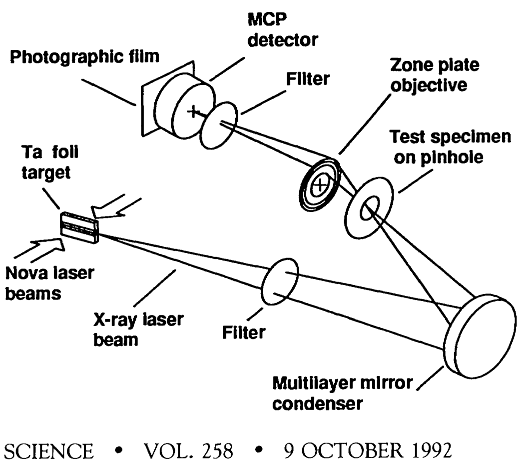

Fig. 1. Schematic of the x-ray microscope showing its main components. MCP, microchannel plate.